X-641-69-357
PREPRINT

NASA TM X- 63644

ON THE INTERPRETATION OF COSMIC X-RAY AND GAMMA RAY SPECTRA PART 1

J. I. TROMBKA

AUGUST 1969

GSFC
GODDARD SPACE FLIGHT CENTER
GREENBELT, MARYLAND

NOT ENOUGH INFO — CANNOT LOCATE OTHER PTS —

X-641-69-357

PREPRINT

ON THE INTERPRETATION OF COSMIC X-RAY AND GAMMA RAY SPECTRA

PART I

J. I. Trombka

August 1969

GODDARD SPACE FLIGHT CENTER

Greenbelt, Maryland

ON THE INTERPRETATION OF COSMIC X-RAY AND GAMMA RAY SPECTRA

PART I

J. I. Trombka

GODDARD SPACE FLIGHT CENTER

Greenbelt, Maryland

ON THE INTERPRETATION OF COSMIC X-RAY AND GAMMA RAY SPECTRA

PART I

J. I. Trombka

ABSTRACT

It is suggested that changes in the slope of a measured distribution may be explained partially by the effect of the measurement process itself. We have developed a method which allows us to determine both the pulse height spectrum from a known photon spectrum, and the photon spectrum from a measured pulse height spectrum. Information derived from these two spectra differs significantly. For example, if, using a 3" × 3" NaI(Tl) detector, we attempt to measure a photon differential energy spectrum characterized by a $V(E) = E^{-1.5}\,dE$ distribution, we obtain a pulse height spectrum with a number of breaks in slope: a -1.5 slope in the energy region up to 60 keV, a -1.7 slope in the energy region up to 300 keV, and a slope of -2.3 from .3 MeV to 2 MeV. The technique for deriving the photon spectra from the measured pulse height spectra eliminates the effects of instrumental response, and further allows for meaningful comparison with data from different detectors.

CONTENTS

ON THE INTERPRETATION OF COSMIC X-RAY AND GAMMA RAY SPECTRA

INTRODUCTION

A number of papers have been published recently that consider the cosmological implication of the diffuse X-ray and gamma ray background.[1-4] Certain breaks in the slope of the measured spectra have been noted, and some theoretical models have been proposed to explain these changes in slope. It is suggested that these changes in slope of the measured distribution may be explained partially by the effect of the measurement process itself.

The measured pulse heights reported are not identical with the true photon spectra (which are of theoretical significance). This is because the response of a real crystal detector to a delta-function photon spectrum is not a delta function pulse height spectrum, but is a characteristic continuous response function describing the energy imparted to the crystal via the various mechanisms to be discussed. For example, Figures 1, 2, and 3 show the characteristic crystal response of NaI(*Tl*) detectors to input photons in the three important energy regions. Figure 1 characterizes the response function around 200 keV. Figure 2 characterizes the response function for energies less than 1 MeV. Figure 3 is characteristic of the response function for energies greater than 1 Mev. There is a transition from one region to another, and we cannot obtain sharply defined limits for the transition.

It is further suggested that before we attempt to compare theory with experiment, with respect to the measured pulse height spectra, the detector effects be eliminated from these spectra. Techniques developed at our laboratory for accomplishing this end will be presented.

RELATIONSHIP BETWEEN PHOTON SPECTRUM AND PULSE HEIGHT SPECTRUM

Information concerning the differential energy photon spectrum is obtained by measuring the interaction of these photons with a detector system. This measured interaction spectrum, or pulse height spectrum,* does not necessarily reflect a one to one correspondence with the photon spectrum. Consider Equation (1).

$$Y(V) = \int_0^{E_{max}} T(E)\ S(E,V)\ dE \qquad (1)$$

where $T(E)$ is the differential energy photon spectrum as a function of (E), $S(E,V)$ is the detector interaction function which reflects the mechanisms of converting photons of energy, E, into a pulse height signal, V, at the output of the detector, and $Y(V)$ is the measured pulse height or interaction spectrum as a function of pulse height, V.

*The term, pulse height, is used to describe the spectra, because the detector output is usually an analog voltage or current signal. This analog signal is digitized using a multi-channel pulse height analyzer.

The information that is desired, in terms of correlating various theoretical models with experimental measurement, is the differential energy photon spectrum, $T(E)$. The problem is to obtain the photon spectrum, $T(E)$, information from the measured pulse height spectrum, $Y(V)$, knowing only the nature of the interaction process, $S(E,V)$.

NATURE OF THE FUNCTION, $S(E,V)$

In order to solve equation (1) for $T(E)$, we must consider the nature of the interaction function, $S(E,V)$. This function depends on the nature of the detector system. Proportional counters, solid state detectors, and scintillation counters are most important among the detectors used in space flight to determine the diffuse gamma ray and X-ray background spectra. In our discussion, we consider the properties of the scintillation detectors. Similar considerations can be carried out both for solid state and proportional counters.

The pulse height spectrum obtained when monoenergetic gamma rays are detected using a scintillation system, is never a line. Its shape is determined by gamma ray energy and source detector configuration. The shapes of these monoenergetic pulse height spectra are primarily determined by:

1. The relative magnitude of the photoelectric absorption, Compton scattering, and pair production cross sections; and,
2. The losses and statistical fluctuations that characterize the crystal, light collection, and photomultiplier system.[5]

Let us examine the case where photoelectric absorption predominates, and Compton scattering and pair production are thought to be negligible. In this process, the kinetic energy imparted to a secondary electron is equal to the energy of the gamma ray minus the electron binding energy. This binding energy can be reclaimed in terms of the scintillation process by the absorption of the X-rays produced after photoelectric absorption. There is also the possibility that the X-rays may escape the crystal without being absorbed. The pulse height distribution caused by photoelectric absorption is characterized by two regions: the region of total absorption (the photopeak), and the region of total absorption minus X-ray escape energy (the escape peak). This distribution spreading, plus the Gaussian spreading previously discussed, yields a pulse height spectrum similar to that shown in Figure 1.

When Compton scattering becomes an important energy loss mechanism, another region, the so-called Compton continuum, is observed in the pulse height spectrum. In terms of the scintillation process, all the energy lost in scattering will be given up to the electron as kinetic energy. The gamma ray may lose part of its energy to the crystal; furthermore, after suffering a Compton collision or a number of Compton collisions, it may suffer a photoelectric absorption and lose its remaining energy. Thus the gamma ray either loses all of its energy in the crystal, or loses part of its energy in the crystal while the remainder of the ray escapes the crystal at a diminished energy. See Figure 2.

At energies higher than 2 MeV, pair production becomes appreciable. Two false "photopeaks" are then observed. Figure 3 is the pulse height spectrum of Na^{24}. The gamma ray energies emitted by Na^{24} are 2.76 MeV and 1.38 MeV. The three peaks of greatest pulse height are caused, in order of increasing pulse height, by:

1. Pair production with escape of both annihilation quanta;
2. Pair production with the absorption of one annihilation quantum;
3. Pair production with absorption of both annihilation quanta, and total absorption by photoelectric effect or any combination of other effects leading to total absorption.

In addition to the photopeak, the iodine X-ray escape peak, the Compton continuum, and the pair escape peaks, there are a number of other regions characteristic of experimentally determined monoenergetic pulse height spectra. These are:

1. The multiple Compton scattering region: Because of such scattering from materials surrounding the source and crystal, thus degrading the primary energy, there is a continuous distribution of gamma rays incident upon the crystal with energies less than the maximum energy. This tends to spread out the true Compton continuum produced by gamma rays of undegraded energy scattering in the crystal.
2. Annihilation radiation from the surroundings: Positrons emitted from the source may annihilate the surrounding material. Some of the 0.51

MeV gamma rays produced in such a manner will reach the crystal, and a pulse height spectrum characteristic of 0.51 MeV gamma rays will be superimposed on the monoenergetic pulse height spectrum (see Figure 4).

3. Coincidence distribution: If two gamma rays interact with the crystal during a time which is shorter than the decay time of the light produced in the scintillation process, a pulse will appear whose height is proportional to the sum of energies lost to the crystal by both interacting gamma rays (see Figure 5).

Because the interaction time of both single and multiple interactions is shorter than the decay time of the light in the crystal, a single gamma ray interacting with the crystal produces only one pulse. The magnitude of the pulse height is affected by the type or number of interactions for a given gamma ray. Thus, if the above-mentioned coincidence effects are negligible, the measured monoenergetic pulse height spectrum can be considered as a distribution of the probability of energy loss as a function of energy for the given gamma ray energy and geometrical configuration. In addition, the shape of the monoenergetic pulse height distribution depends on the source detector geometry.

NUMERICAL SOLUTION

The problem of the analysis of gamma ray pulse height spectra in this particular spectral region lies in the fact that we cannot yet perform this inverse transform analytically. Numerical methods must therefore be used.

The first step in the development of a numerical method is to show that the integral in equation (1) can be written as a sum of discrete components. Remember also that T(E) is not a discrete distribution in energy, but (in terms of the observations we are interested in) a continuous energy distribution. The following technique for obtaining T(E) is based on a theorem in sampling theory,[6-8] and upon the fact that there is a finite energy resolution of the detection system. If a distribution has no oscillatory component with a frequency greater than f_{max}, then, the Shannon Sampling Theorem asserts, samples at discrete points not further apart than $1/2\, f_{max}$ describe the original function exactly. The original function, in fact, may be reconstructed from the samples.[7] If this theorem is applicable, equation (1) can be written as:

$$Y_i = \sum_j T_j \, S_{ij} \tag{2}$$

where Y_i is the measurement of Y(V) in channel or pulse height V, T_j is the total number of gamma rays in energy group ΔE_j about E_j, and S_{ij} is the value of the jth standard spectrum in channel i. The S_{ij} components are, for example, the response of a NaI(*Tl*) detector to an incident monoenergetic gamma ray.

The sampling functions S(E,V) are written as arrays of numbers, S_{ij}. The characteristic shapes of these distributions are shown in Figures 1-5. Considering only the energies where pair production is negligible, these spectra can be described by a Compton continuum and the photopeak. The Compton continuum

is a more slowly varying function than is the photopeak. As a first approximation, the photopeak can be described by a Gaussian equation,

$$y(x) = N \exp - \left[\frac{x^2}{2\sigma_m^2} \right] \tag{3}$$

where $x = (V - V_m)$ in pulse height units, V_m is the pulse height corresponding to energy, E_m, and σ_m is the standard deviation and a function of V_m.

It is further assumed that $y(x)$ is negligible and/or equal to zero for those values of pulse height where $y(x) = N \times 10^{-3}$ in Equation (3). This assumption does not affect the analysis significantly, because these values of $y(x)$ will be lost in the noise (background) of the system.

Finally, it is assumed that the Gaussian Equation (2) can be closely approximated by a $\cos^2 kx$ distribution, i.e., that the amplitudes of the higher frequencies are negligible in terms of the analysis (the comparison is shown in Figure 6). Then the frequency of oscillation or rate of change of shape of the photopeak (response function S_{ij}) is determined in the following manner:

The value of k is chosen so that for $x = 0$, and for $x = \sqrt{2}\,\sigma_m$ (i.e., the e^{-1} on the Gaussian), the amplitudes of the Gaussian and $\cos 2kx$ function are equal. We assume that $N = 1$ in the equation (3), and k is found to be equal to $\pi/4.86\sigma_m$. The frequency, f, can be found in this manner:

$$\cos^2 kx = \frac{1}{2}(1 + \cos 2kx). \tag{4}$$

The frequency is, therefore,

$$f = \frac{2k}{\pi} = \frac{1}{2.43\sigma_m}. \tag{5}$$

The photopeak is assumed to contain the oscillatory component with the maximum frequency. This is the frequency found in equation (5). It is now possible to relate this frequency to the total width at half maximum, $W_{1/2}$. From Equation (3), with $y = N/2$ when $x = W_{1/2}$, then:

$$\sigma_m = \frac{W_{1/2}}{2.35}. \tag{6}$$

Substituting this value of σ_m into Equation (4), the maximum frequency, f_m, is found in terms of $W_{1/2}$:

$$f_m = \frac{.1}{1.03\ W_{1/2}}. \tag{7}$$

For all practical purposes, therefore, the maximum frequency is inversely proportional to the total width at half maximum. The criteria for the maximum separation (M.S.) between sampling components to be used in Equation (3) can then be found using Shannon's Sampling Theorem,

$$\text{M.S.} = \frac{1}{2f_{max}} \simeq 1/2W_{1/2}. \tag{8}$$

The sampling components should be chosen so that their separation in energy will be no greater than the half width at half maximum of their photopeaks. Thus, from information theory, it has been shown that the integral given in Equation (1) can be described as a sum of discrete energy components which describe an energy interval, ΔE, about a given E; and that the energy intervals between the ΔE samples will be no greater than $1/2W_{1/2\,max}$, the half width at half maximum of the photopeak for the function, $S(E,V)$. In this way, the approximation formula, Equation (2), is obtained. Equation (2) is now in a form where a valid numerical transformation can be obtained using techniques derived from the analysis of variance. The details of this derivation can be found in References 9 and 10. Briefly, using the least square principle, the method requires that:

$$M = \sum_j \omega_i \left(Y_i - \sum_j T_j S_{ij}\right)^2 \tag{9}$$

be a minimum, where ω_i is the statistical weight corresponding to the measurement of Y_i in channel i, and $\omega_i = 1/\sigma_{i^2}$ (where σ_{i^2} is the variance of the count in channel i). The other terms have been defined. The partial derivatives of M are taken with respect to T in order to determine the minimum. The solution in matrix form is given by Equation (10).

$$T = (\tilde{S}\,\omega\,S)^{-1}\,\tilde{S}\,\omega\,Y\,, \tag{10}$$

where Y is a vector describing the pulse height spectrum, S is an $m \times n$ matrix describing the discrete set of detector response function using the selection rule derived above, $\tilde{S}$ is the transposition of S, ω is a square diagonal matrix of the weighting functions, and T is a best estimate of the differential energy photon spectrum.

A semi-empirical method is used to derive the function, S_{ij} . This method is described in detail in Reference 11.

Two types of calculation are now available to us. If we know the differential energy photon spectrum, T(E), the expected pulse height spectrum can be obtained using Equation (2). On the other hand, the best estimate of T(E) can be obtained from the measured pulse height spectrum, Y(V) , using Equation (10). Algorithms for finding such solutions are described in References 8, 9, and 10. The use of both methods will be discussed in the next section.

PULSE HEIGHT AND PHOTON SPECTRA

We will now present a number of illustrations to show the nature of the problem, and solutions that can be obtained. Let us assume that we are trying to measure a photon spectrum, T(E), which can be described by a differential energy distribution, $T(E)\,dE = E^{-1.5}\,dE$. Figure 7a shows such a distribution, and T(E) dE is indicated.

The spectrum is measured using a 3" × 3" NaI(*Tl*) crystal. The pulse height spectrum, Y(V) dE , that would be obtained using Equation (2) is indicated in Figure 7a. If we attempt to determine the slope of the line of the pulse height

spectrum, we find the slope to be $Y(V)\,dV = V^{-2.3}\,dV$; significantly different from $T(E)$. Further, if we measure the pulse height spectrum only in the region up to about 60 keV, $Y(V)\,dV = V^{-1.5}\,dV$. If we measure the spectrum from 100 to about 300 keV, $Y(V)\,dV = V^{-1.7}\,dV$, and $Y(V)\,dV = dV^{-2.3}\,dE$ if we determine the slope from 300 keV to 2 MeV. Of course the shape of $Y(V)$ will depend on the size of the detector used, the resolution of the detector, the angular distribution of the incident flux, and other factors. What becomes even more important is, that if we assume that superimposed upon this power law distribution is some type of distribution like the photon inelastic scattering process proposed in Reference 1 (Figure 7b), there is a deviation of $T(E)\,dE$ from the power law distribution at higher energies. The problem that occurs is that the detection system damps out this deviation in the photon spectrum, $T(E)$, and we lose the information concerning this power law process if we analyze the pulse height spectrum alone. This damping will depend, again, on such factors as the crystal size, the resolution, and the angular distribution of the incident flux. Thus, it becomes possible to obtain almost any kind of solution if the pulse height spectrum is mistakenly used for correlating theory with experiment.

The analysis technique that has been developed in our laboratory requires no a priori knowledge of the incident flux for obtaining the solution, $T(E)\,dE$. All that is required is a knowledge of the nature of the interaction process, $S(E,V)$, for the given detector used for the measurement. Figure 8 shows both the meas-

ured pulse height spectrum (a), and the analytically derived photon spectrum (b) obtained using the analytical method just described.

The measured pulse height spectrum (Figure 8a) was obtained during a balloon flight at approximately 100,000 feet, using a 3" × 3" NaI(Tl) detector.[12] The 0.51 MeV annihilation ray peak is easily recognized in the pulse height spectrum. Without assuming any a priori knowledge of the incident photon spectrum, the numerical transformation was performed and the photon spectrum obtained. After the numerical analysis, two other discrete lines became more distinct above background. These lines were later identified as the potassium 40 (K-40) line caused by the presence of this material in the atmosphere, and the magnesium (Mg-24) line which can be attributed to excitation induced by the incident cosmic ray flux on the gondola structural material. Once identified, these discrete lines could be subtracted from the total photon spectrum to obtain the pure continuous spectrum.

The photon spectrum (Figure 8b) can be used to reconstruct the pulse height spectrum (Equation 2). The results are shown in Figure 8a. As can be seen, it is almost impossible to differentiate between the two curves.

Finally, in Figure 8b, we see that the last two points are higher than the continuum. These two points contain information of all the energies striking the crystals with energies greater than that observed in the measured energy region. These so-called "end effects" will occur when only parts of the total spectrum are analyzed.

DETECTOR SIZE

We can generalize this discussion to consider the effects of detector size and resolution. These factors can greatly affect the shape of the pulse height spectra. Calculations of pulse height spectra obtained by using smaller crystals have been carried out in our laboratory. The major noticable effect is a steepening of the slope of the curve, and the breaks in slope, that occur at lower energies, of the pulse height spectrum. This steepening, and the changes of break in slope, can be attributed mainly to two factors: decrease in detection efficiency, and increase in the size of the Compton region as compared to the photopeak region characteristic of the crystal response function. The latter result indicates that sensors with minimum contributions of the Compton continuum are the most consequential for measuring the continuous photon spectrum. Thus, even though the energy resolution is significantly better with small solid state detectors (e.g., Ge (Li)), we would choose a large scintillation detector (e.g., NaI(Tl)) with a significantly lower Compton continuum contribution to measure a continuous photon spectrum. On the other hand, if we wish to determine discrete energies above the background, we will sacrifice the reduced Compton for the improved resolution of the solid state detectors.

SUMMARY

We have described a method which allows us to determine both the pulse height spectrum from a known photon spectrum, and the photon spectrum from a measured pulse height spectrum. Information from these two spectra differs

significantly. For example, if, using a 3" × 3" NaI(Tl) detector, we attempt to measure a photon differential energy spectrum characterized by a $V(E) = E^{-1.5}\,dE$ distribution, we obtain a pulse height spectrum with a number of breaks in slope: a -1.5 slope in the energy region up to 60 keV, a -1.7 slope in the energy region up to 300 keV, and a slope of -2.3 from .3 MeV to 2 MeV. The information of most interest is that which can be derived from the photon spectrum. The technique for deriving the photon spectra from the measured pulse height spectra eliminates, in a sense, the effects of instrumental response. It further allows for meaningful comparison with data from different detectors.

In a future paper (Part II), this method will be used to correlate the data obtained from a variety of experimenters in order to obtain a valid photon spectrum over the energy region 10 keV to 10 MeV. A joint effort by the author and Dr. F. Stecker is underway to collect the data, perform the analysis, and appraise the theoretical applications of the resultant spectrum.

ACKNOWLEDGMENT

We thank F. Stecker of the Theoretical Studies Branch, Goddard Space Flight Center, for his help and advice in the preparation of this paper; R. Schmadebeck, of the same branch, for help in the development of the computer programming necessary to perform the least square analysis; and Sabinus H. Christensen, Lincoln University (Pa.), for his help and review of this paper.

REFERENCES

1. Stecker, F. W., Proc. I.A.U. Symposium No. 37 on Non-Solar X- and Gamma Ray Astronomy, Rome (1969), to be published:

   Stecker, F. W., and Silk, J., Nature, 221, 1229 (1969).

2. Silk, J., and McCray, R., Astrophysical Letters, 3, 59 (1969).

3. Felton, J. E., and Rees, M. J., Nature, 221, 924 (1969).

4. Silk, J., Nature, 221, 348 (1969).

5. Bell, P. R., "The Scintillation Process," Beta and Gamma Ray Spectroscopy, Ed., Kai Siegbaum, North Holland Publishing Co., Amsterdam (1955).

6. Burrus, W. R., "Unscrambling Scintillation Spectrometer Data," IRE Trans. on Nuc. Sci., INS-7:2-3, (1960).

7. Linden, D. A., "Discussion of Sampling Theorem," Proc. IRE, 47, (1959).

8. Trombka, J. I., "On the Analysis of Gamma Ray Pulse Height Spectra," Dissertation, University of Michigan (1961).

9. Trombka, J. I., and Schmadebeck, R. L., "A Method for the Analysis of Pulse Height Spectra Containing Gain-Shift and Zero-Drift Compensation," Nuclear Instruments, 62, 253-261 (1968).

10. Trombka, J. I., and Schmadebeck, R. L., "A Numerical Least Square Method for Resolving Complex Pulse Height Spectra," NASA SP-3044 (1968)

11. Heath, R. L., Helmer, R. G., Schmittrath, L. A., and Cazien, G. A., "The Calculation of Gamma Rays Shapes for Sodium Iodide Scintillation Spectrometers," IDO-17017, AEC-TID-4500 (April 1965).

12. Peterson, L., Private Communication, University of California, San Diego (1968).

FIGURE CAPTIONS

Figure 1. Sc^{47} gamma rays on 3" × 3" NaI(Tl) crystal. Source at 3 cm.

Figure 2. Cs^{137} gamma rays on 3" × 3" NaI(Tl) crystal. Source at 10 cm.

Figure 3. Na^{24} gamma rays on 3" × 3" NaI(Tl) crystal. Source at 3 cm.

Figure 4. Zn^{65} at 0.24 cm from NaI(Tl) crystal. Source at 10 cm.

Figure 5. Co^{60} gamma rays on 3" × 3" NaI(Tl) crystal. Source at 10 cm.

Figure 6. Comparison of Gaussian distribution with a $\cos^2 kx$ distribution. Fitted at $x = 0$ and $x = \sqrt{2\sigma}$.

Figure 7. (a&b) Effect of detector interaction with incident photon flux in the measurement of gamma rays.

Figure 8a. Pulse height spectrum. 3" × 3" NaI(Tl) crystal atmospheric spectrum.

Figure 8b. Photon spectrum. 1 channel = 14.9 keV.

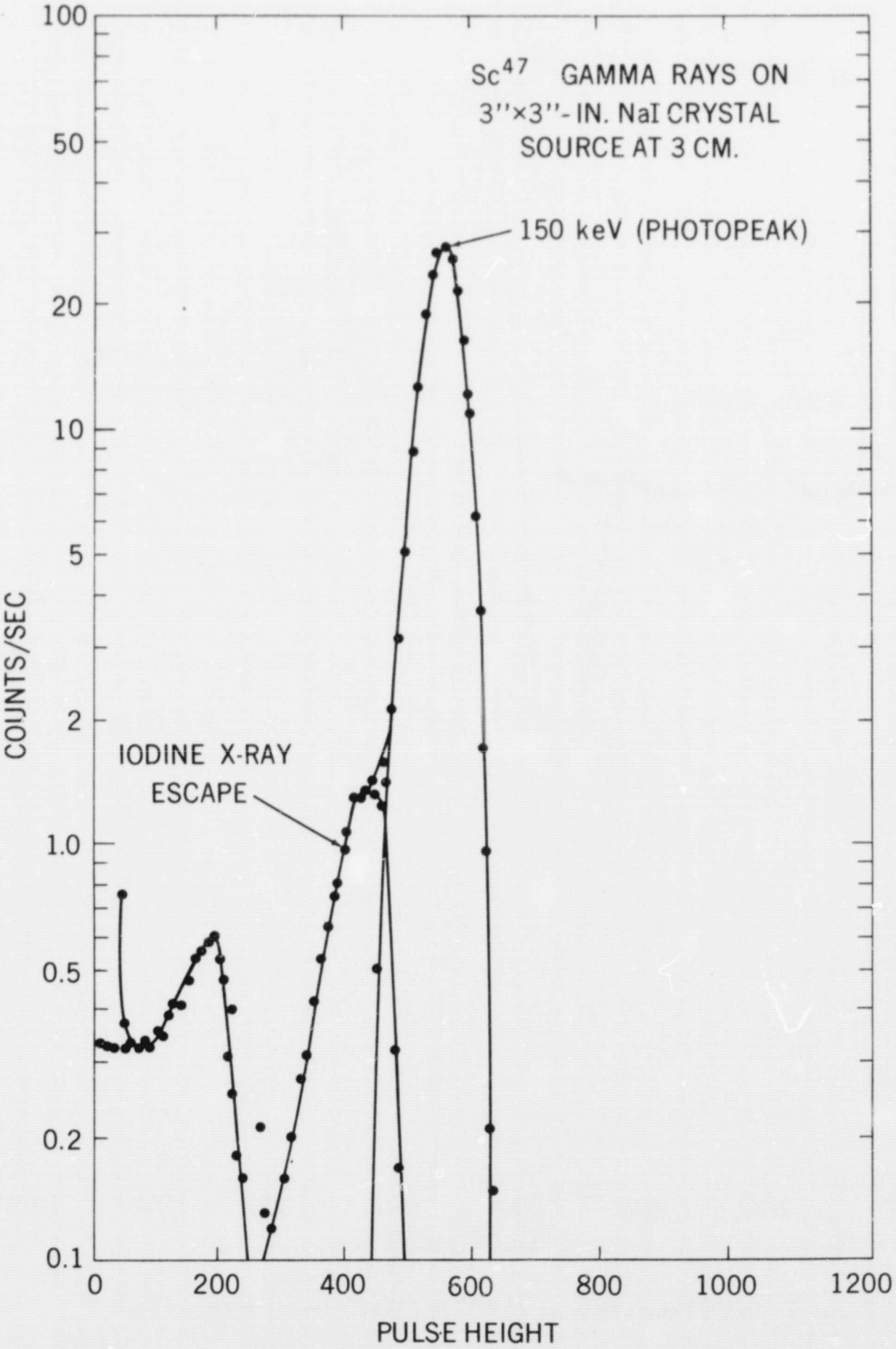

Figure 1. Sc^{47} Gamma Rays on 3" x 3" NaI(Tl) Crystal. Source at 3 cm.

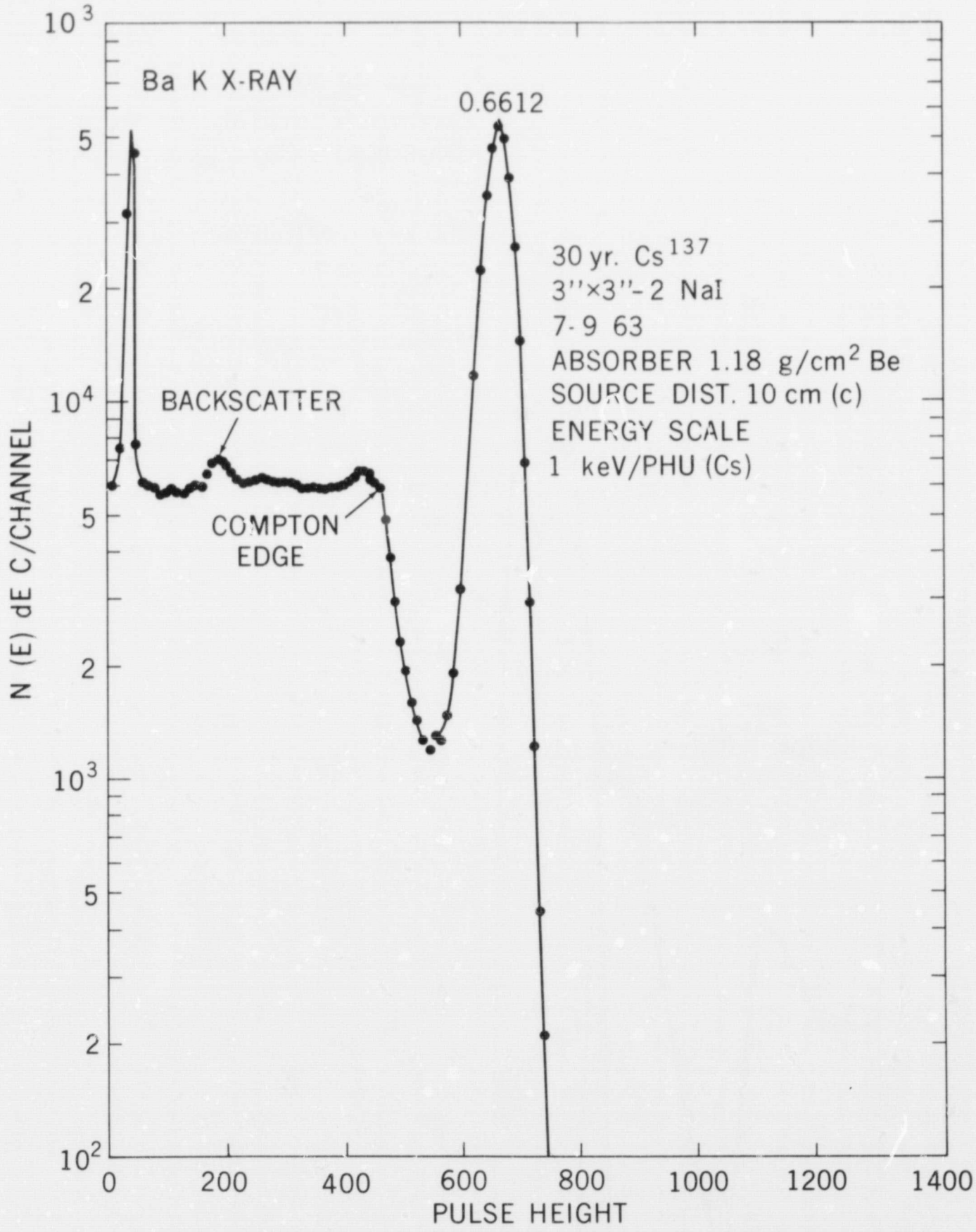

Figure 2. Cs^{137} Gamma Rays on 3" x 3" NaI(Tl) Crystal. Source at 10 cm.

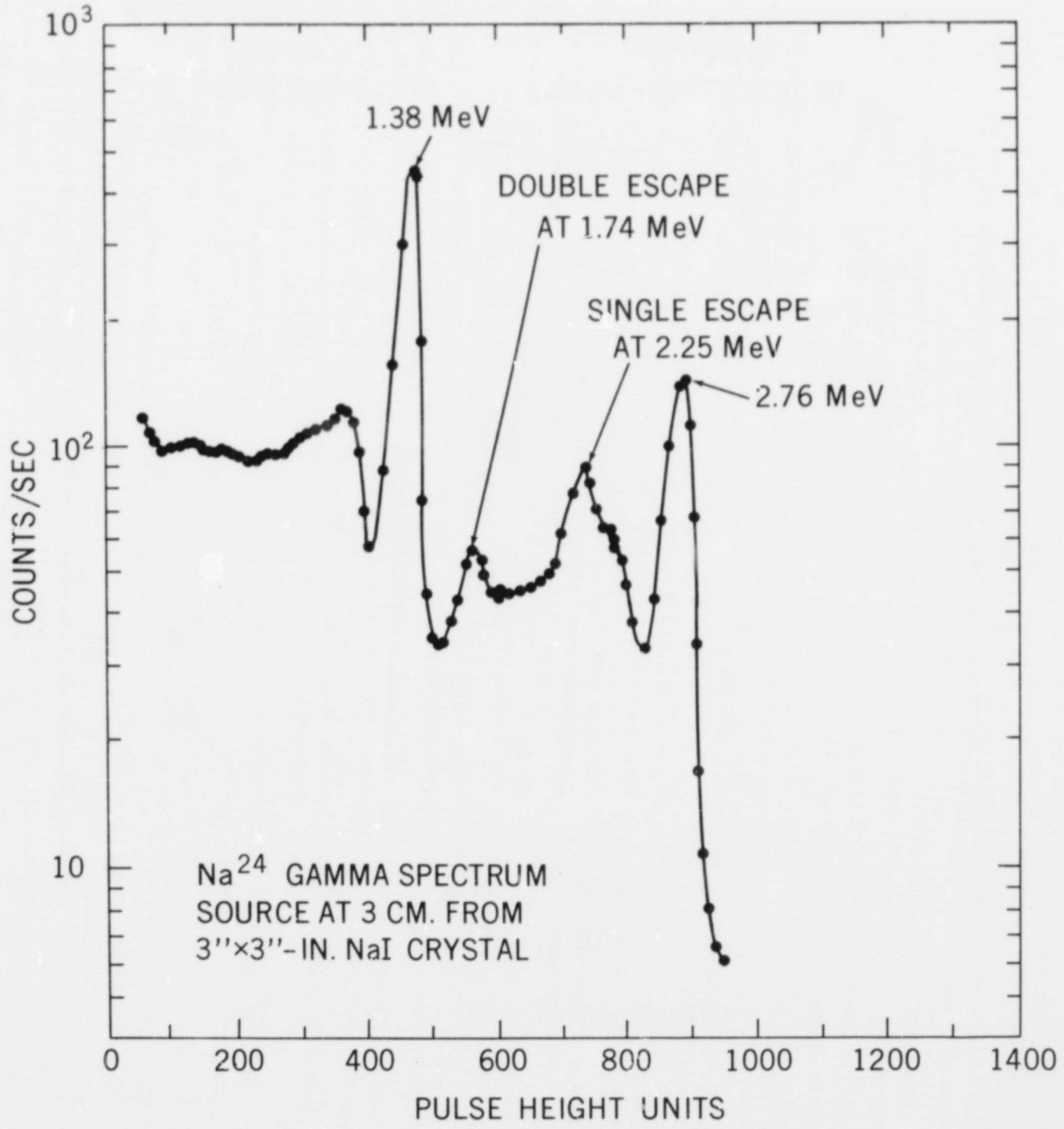

Figure 3. Na^{24} Gamma Rays on 3" x 3" NaI(Tl) Crystal. Source at 3 cm.

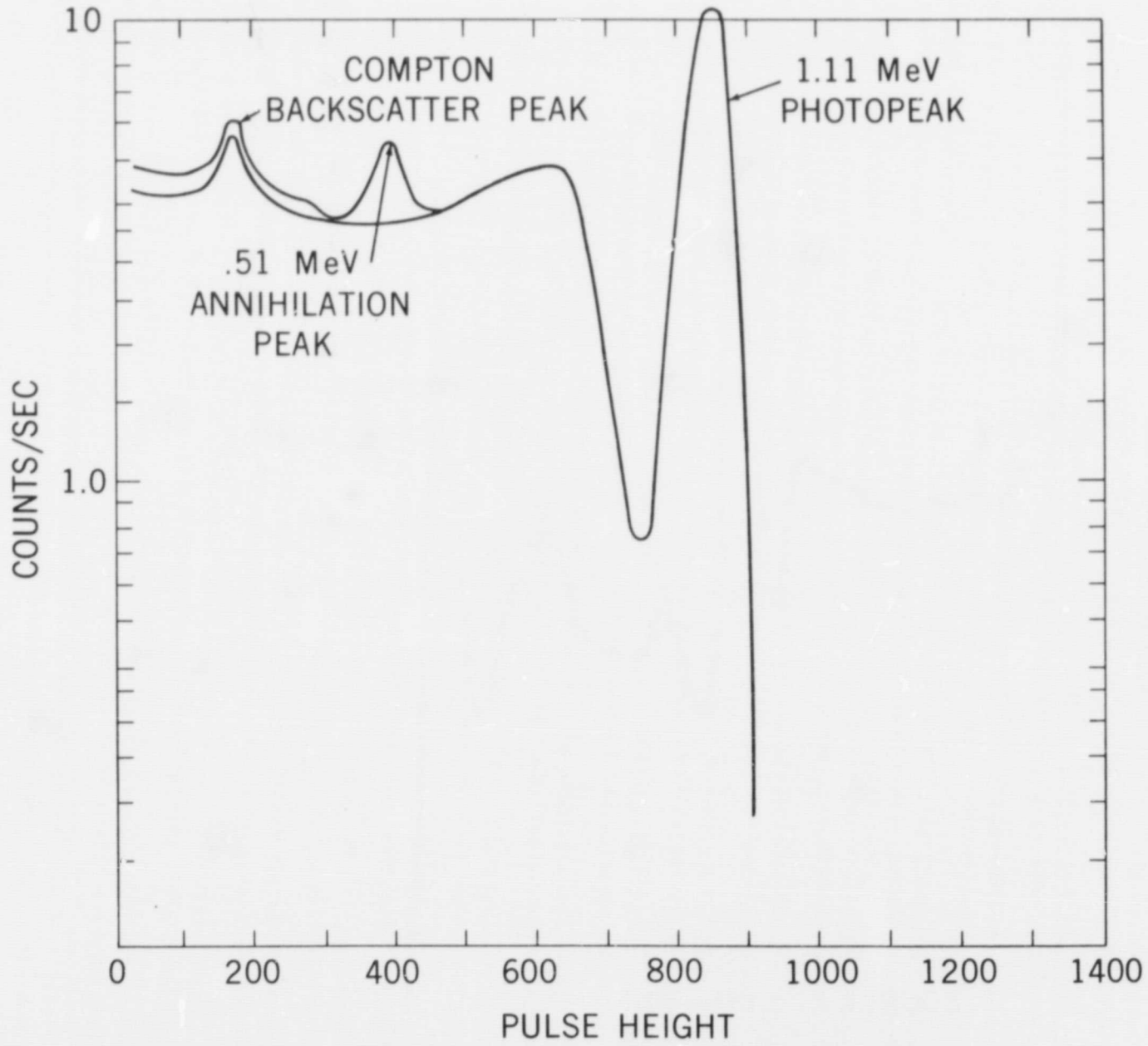

Figure 4. Zn^{65} at 0.24 cm From NaI(Tl) Crystal. Source at 10 cm.

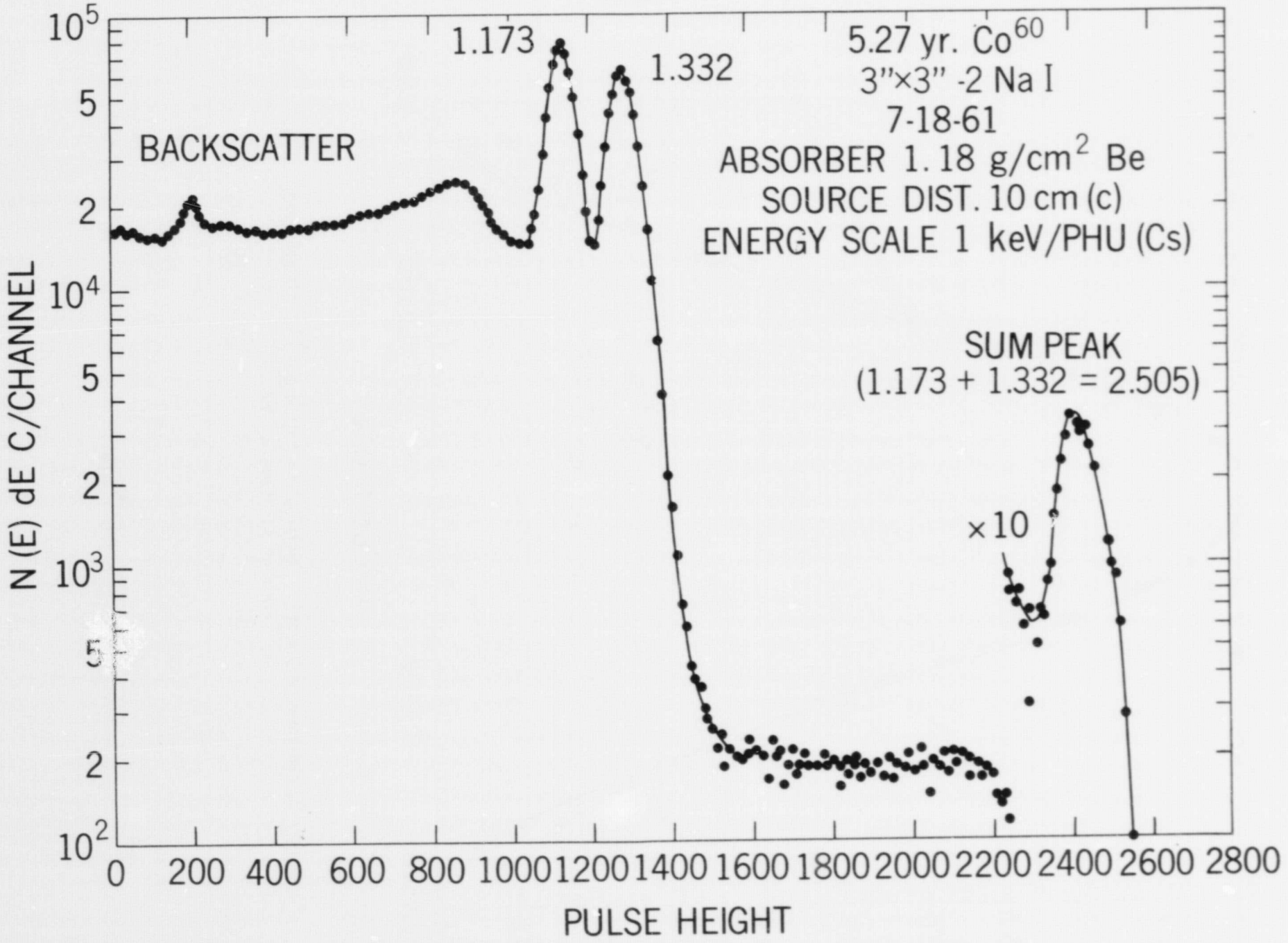

Figure 5. Co^{60} Gamma Rays on 3" x 3" NaI(Tl) Crystal. Source at 10 cm.

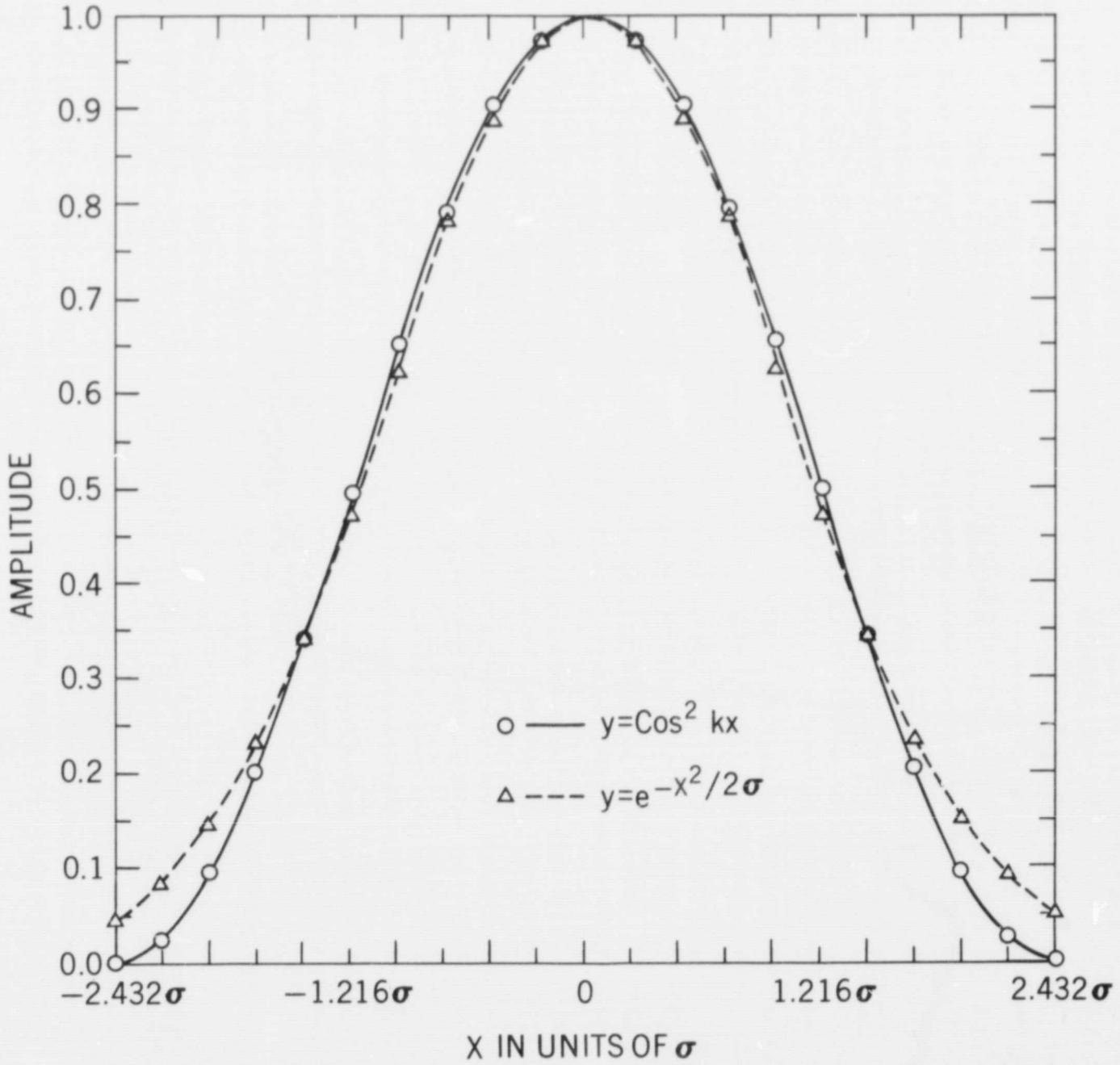

Figure 6. Comparison of Gaussian Distribution With a $\cos^2 kx$ Distribution. Fitted at $x = 0$ and $x = \sqrt{2}\,\sigma$.

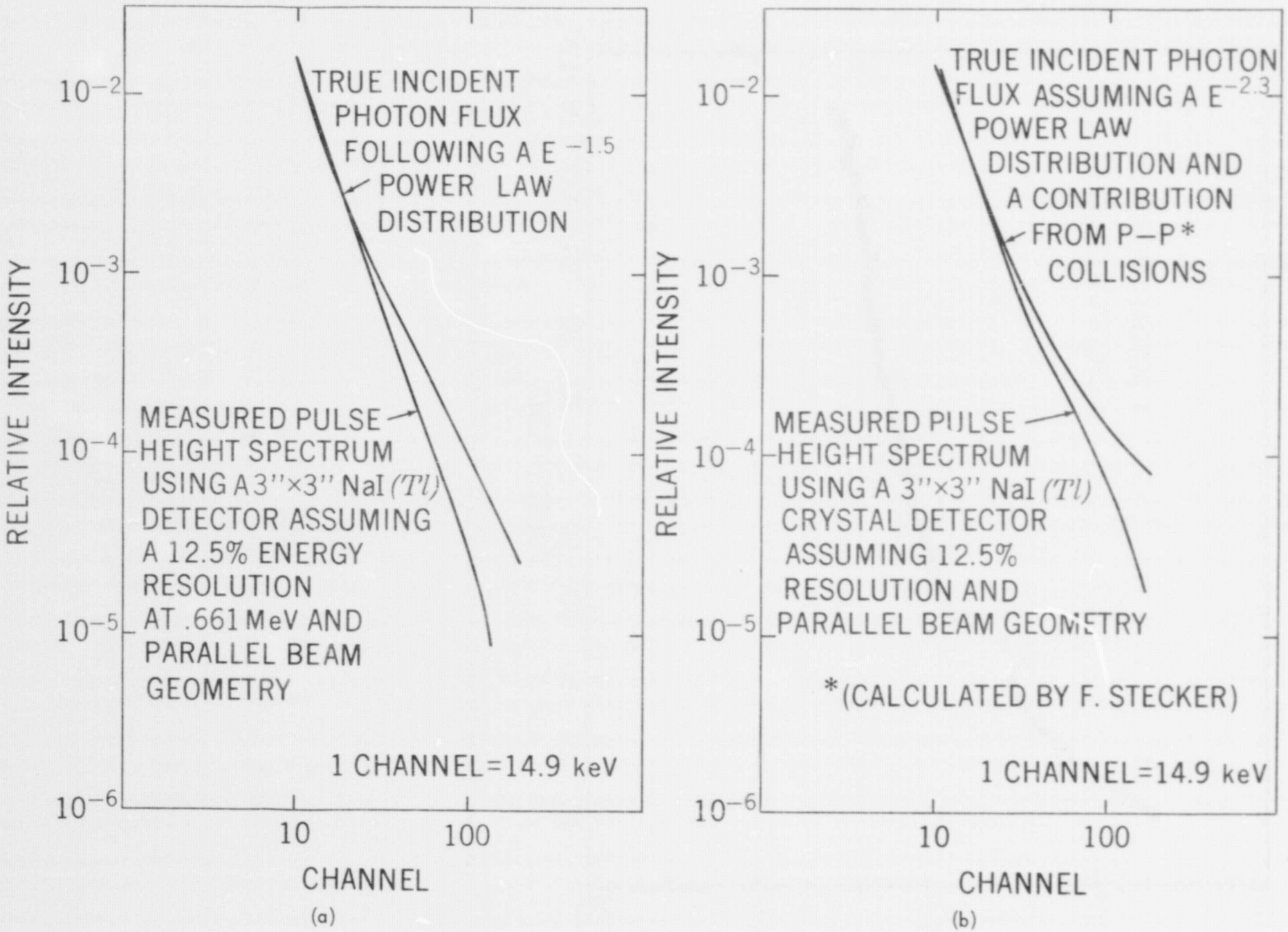

Figure 7. Effect of Detector Interaction With Incident Photon Flux in the Measurement of Gamma Rays.

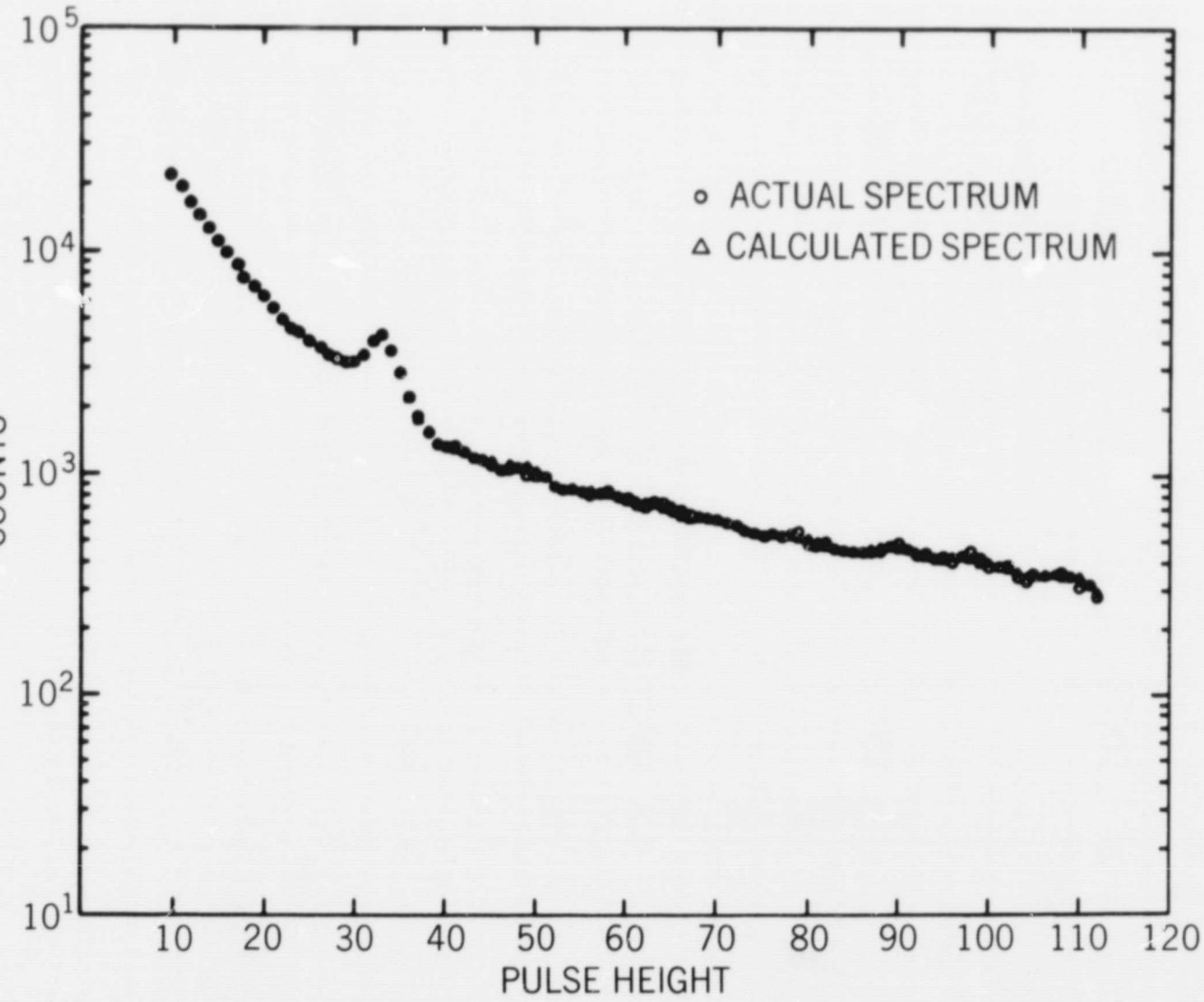

Figure 8a. Pulse Height Spectrum. 3" x 3" NaI(Tl) Crystal Atmospheric Spectrum.

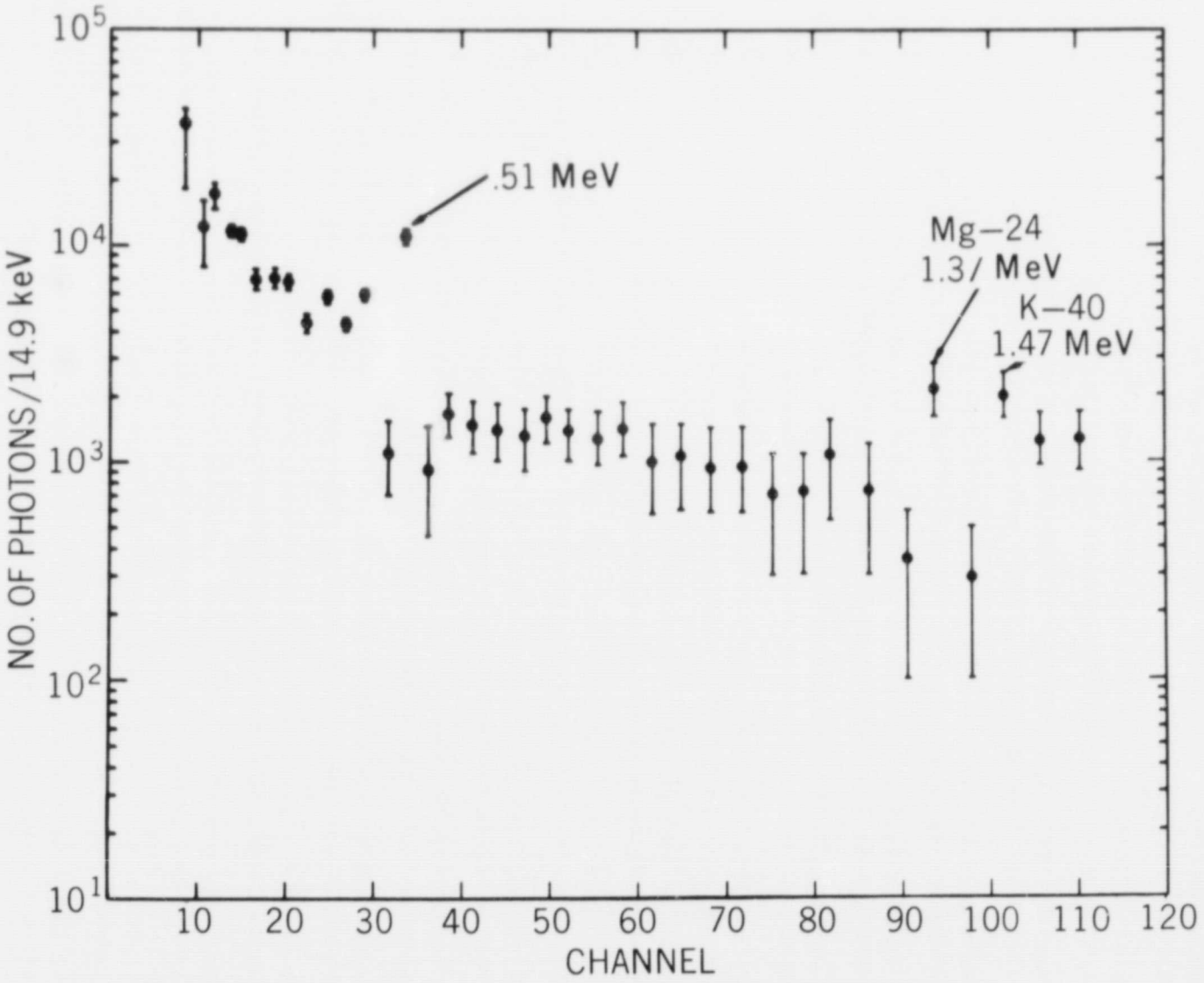

Figure 8b. Photon Spectrum. 1 Channel = 14.9 keV.